



Feature Article

Chain statistics in polyethylene crystallization

Giuseppe Allegra*, Antonino Famulari¹

Politecnico di Milano, Dipartimento di Chimica, Materiali e Ingegneria Chimica "G. Natta", via Mancinelli 7, 20131 Milano, Italy

ARTICLE INFO

Article history:

Received 11 November 2008

Received in revised form

14 January 2009

Accepted 20 January 2009

Available online 7 February 2009

Keywords:

Polymer physics

Chain statistics

Polyethylene crystallization

ABSTRACT

The molecular mechanism of polyethylene crystallization in solution is revisited within the framework of the bundle model [Allegra G, Meille SV. *Adv Polym Sci* 2005;191:87]. Previous SANS/IANS results [Sadler DM, Keller A. *Science* 1979;203:263; Spells SJ, Sadler DM. *Polymer* 1984;25:739; Stamm M, Fischer EW, Dettenmaier M, Convert P. *Faraday Disc Chem Soc* 1979;68:263] from partially deuterated samples are used. It is proposed that the chain deposits on the growing lamella under the form of compact crystalline domains, their size being $\cong \sqrt{M_w}$. The radius of gyration of the crystallized chain agrees with a model consisting of a linear sequence of crystalline domains connected by chain segments with random orientations. It is suggested that the whole chain is in a bundle meta-stable equilibrium and collapses in the vicinity of the growing lamellar edge, then crystallizing around secondary nuclei. Compactness of the crystalline domains is correlated to prior chain collapse in the liquid state. The observed proportionality to $\sqrt{M_w}$ of the crystalline domain size is approximately explained.

© 2009 Elsevier Ltd. Open access under [CC BY-NC-ND license](http://creativecommons.org/licenses/by-nc-nd/3.0/).

1. Introduction

The molecular mechanism of polymer crystallization has been the subject of a considerable debate in the last decades. Whether from the melt, from solution or from the glass, under flux or under quiescent conditions, the issue of polymer crystallization has attracted much interest, both for its scientific and for its technological aspects [1–3]. An increasingly large body of experimental results [4–26] has been investigated through theoretical and simulation approaches, frequently complementing one another [10,11,27–53].

We shall concentrate on a few aspects inherent with quiescent crystallization of linear polyethylene from solution, that may be summarized by the question: What is the molecular mechanism of polyethylene crystallization in solution?

In the following, after reviewing concisely some relevant experimental information (Section 2), we provide elements to clarify that question. In Sections 3 and 4 we revisit the “bundle model” previously proposed by some of us [30–33], and in Section 5 we illustrate the molecular mechanism of crystallization from the bundle state of the chain. After a general discussion (Section 6) where structural proposals from other Authors are comparatively

reviewed [2–9,19,22,23,35–39,48], concluding remarks follow (Section 7).

2. SANS/IANS diffraction data from solution-crystallized samples: model and structural considerations

The following results were obtained by two Groups of Authors, both of them by SANS–IANS neutron scattering on partially deuterated, un-fractionated polyethylene samples (M_w/M_n roughly around 2) with different molecular weights M_w . All the samples were crystallized at 60–70 °C from *o*-xylene solutions.

In Fig. 1 we show the “stacked-sheet” model proposed by Stamm, Fischer et al. and the corresponding comparison between experimental and calculated diffraction plot; the calculations were carried out by the same Authors [9]. In Fig. 2 we show a similar comparison of Kratky plots obtained by Spells and Sadler [7] from 4 samples with different molecular weights, with the diffraction spectra calculated by us (see Appendix A) from “stacked-sheet” models analogous to those of the previously quoted Authors [9]. Fig. 3 gives the SANS radius of gyration (R_g) from melt- and solution-crystallized, partially deuterated samples [4–8]; the solution results are dominated by the chain dimensions parallel to the plane of the lamellae [5]. The experimental results reported in Figs. 1–3 will represent the basis of our following analysis.

In Fig. 2, the stem arrangements (domains) shown in the right-hand side are to be regarded as averages; each chain is assumed to consist of spatially uncorrelated domains. Consistent with the observed fold length of about 100 Å for this undercooling degree

* Corresponding author. Tel.: +39 0223993023; fax: +39 0223993081.

E-mail addresses: giuseppe.allegra@polimi.it (G. Allegra), antonino.famulari@polimi.it (A. Famulari).¹ Tel.: +39 0223993044; fax: +39 0223993081.

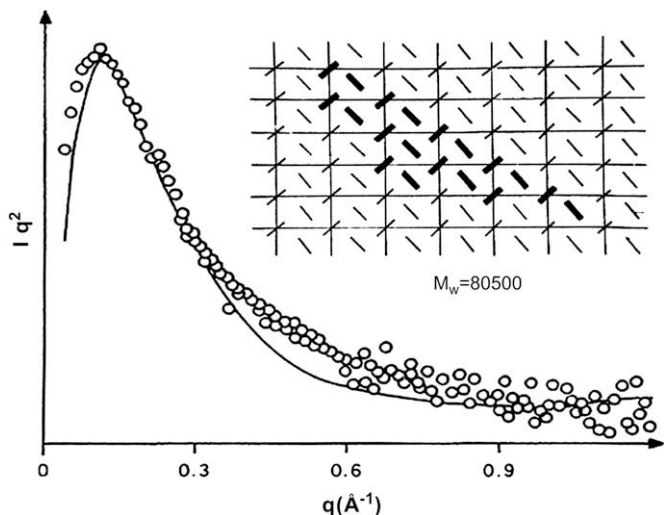


Fig. 1. Kratky plot from a partially deuterated polyethylene sample and corresponding structure of the crystalline domain, as seen parallel to the stem axis. The labelled chain is shown in heavy lines. (Taken from Ref. [9], authors Stamm, Fischer, Dettenmaier, Convert).

($\Delta T = T_0 - T_C \sim 45^\circ\text{C}$, T_0 ideal melting temperature, T_C temperature of crystallization [31]), each stem is a rod-like sequence of ($-\text{CH}_2-\text{CH}_2-$) groups and is assumed to comprise about 80 C atoms; all the stems are placed at the same height with respect to a horizontal plane. The procedure to calculate the diffraction intensity is given in Appendix A.

As shown in Figs. 1 and 2, all the diffracting domains – henceforth (chain) crystalline domains – display a roughly similar shape, the ratio between their average thickness and width showing a modest increase with increasing overall size. Both the small distance from the chain axis of the diffracting H and D atoms and the small deviation from hexagonal symmetry of the stem axes in the orthorhombic unit cell, turn out to be essentially irrelevant on the diffraction results in the range $0 \leq q (= (2\pi \sin \theta)/(\lambda)) \leq 0.25 \text{ \AA}^{-1}$. The average direction of elongation of the domains is parallel to the crystallographic direction (110) for orthorhombic PE [4]. We see that n_{stem} does not increase in a direct proportion with the molecular weight M_w . Fig. 4 shows a double-logarithmic plot of M_w vs. q_{max} , showing an approximate linear dependence, leading to the following power law:

$$(q_{\text{max}})^{-2} \propto n_{\text{stem}} \cong 0.22 \cdot M_w^\alpha; \quad \alpha = 0.50 \pm 0.03. \quad (1)$$

Notice that the (approximate) shape similarity among the Kratky plots, suggesting analogous similarity among the crystalline chain domains is exploited, suggesting $(q_{\text{max}})^{-2} \propto n_{\text{stem}}$; we point out that $(q_{\text{max}})^{-2}$ has the dimensions of a surface and n_{stem} is proportional to the domain area projected along the stem axis. Eq. (1) may be summarized by

$$n_{\text{stem}} \approx \sqrt{M_w} \quad (1')$$

It should be stressed that n_{stem} is an average for the particular M_w . Eq. (1) is independently validated by the following comparison among the calibrated peak intensities shown in Fig. 2. Let us first divide the Kratky peak intensity Iq^2_{peak} by Iq^2_{stem} , or the intensity diffracted by a single stem at the same q ; we thus obtain the peak intensity diffracted from material points lying in a plane approximately orthogonal to the stem axes, each point replacing a whole stem. As shown theoretically by Guinier [20] and experimentally

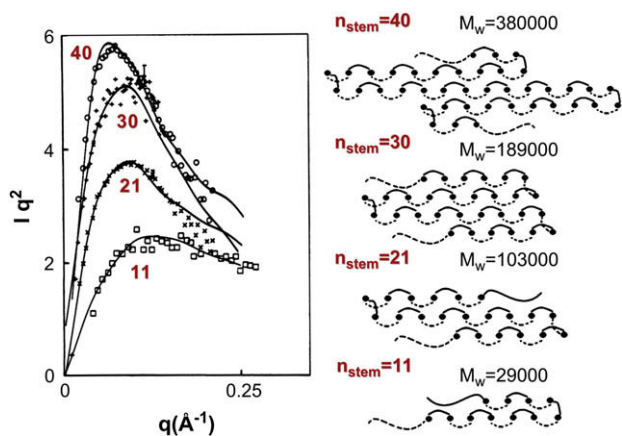


Fig. 2. Comparison between experimental Kratky plots reported by Spells and Sadler [7] from partially deuterated PE samples and the diffraction spectra calculated assuming the crystalline domain structures reported at right (see Appendix A for the calculations).

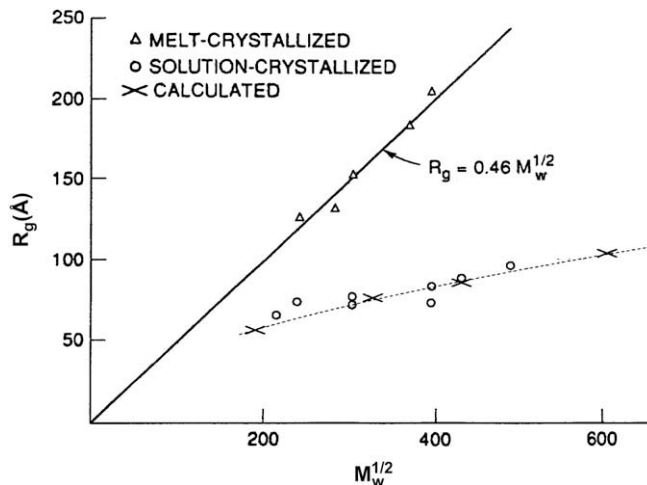


Fig. 3. SANS radius of gyration (R_g) from melt- and solution-crystallized, partially deuterated samples (solution data taken and reported by Sadler, Keller, Spells, see Refs. [4–8]). Note the difference between melt-crystallization (unperturbed chains) and solution crystallization (unperturbed chains).

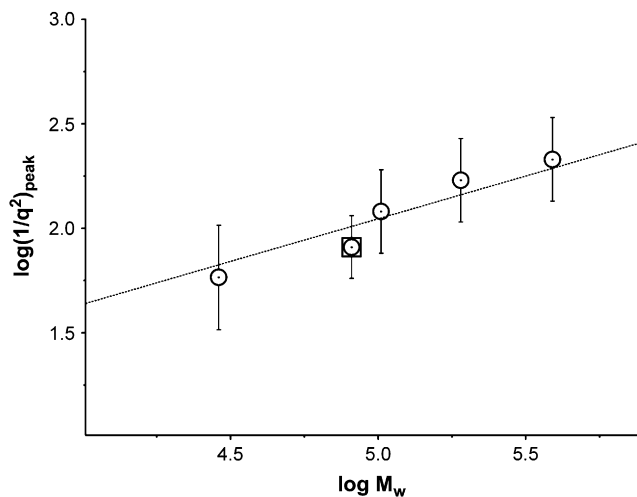


Fig. 4. Correlation between the q -coordinate at the peak of the Kratky plot, and M_w , from Figs. 1 and 2. The experimental point enclosed in a square is from Fig. 1 (Ref. [9]), the other points from Fig. 2 (Ref. [7]). Error bars are shown.

Download English Version:

<https://daneshyari.com/en/article/5186314>

Download Persian Version:

<https://daneshyari.com/article/5186314>

[Daneshyari.com](https://daneshyari.com)